ELECTRICAL SIGNATURE ANALYSIS (ESA) AS A DIAGNOSTIC MAINTENANCE TECHNIQUE FOR DETECTING THE HIGH CONSEQUENCE FUEL PUMP FAILURE MODES

D. E. Welch, H. D. Haynes, D. F. Cox, and R. J. Moses
Oak Ridge National Laboratory

Project Background and Technology Base

C-141 Background Description and Technology Need: The mission capable status of the C-141 cargo aircraft depends on many systems, one of which is the fuel delivery system. Fuel is delivered to the C-141 engines from the wing fuel tanks by means of twenty centrifugal fuel boost pumps, one primary and one secondary in each tank [four main tanks, four auxiliary tanks, and two extended range (ER) tanks]. The primary and secondary fuel boost pumps are submerged inside the wing fuel tanks. They operate on 115/200 VAC, 3-phase electrical current. The main fuel booster pump (Figure 1) is deployed in the main tanks; the auxiliary fuel booster pump (Figure 2) is installed in the auxiliary and ER tanks.

Figure 1: *C-141 main fuel booster pump.*

Figure 2: *C-141 auxiliary fuel booster pump.*

Presently, these fuel pumps are removed and replaced in the event of failure; failed pumps are routed to the Oklahoma City Air Logistics Center (OC-ALC) for repair. When a failure occurs, a significant out-of-service time occurs for the aircraft due to the need to order and receive replacement parts before repairs can be completed.

During recent experience, failure of fuel system booster pumps has accounted for over 4000 hours of aircraft unscheduled downtime per year. This equates to one aircraft being unavailable for nearly half a year. On average, the loss of airlift for this many days has a potential multi-million dollar negative impact annually on the Air Mobility Command's Transportation Working Capital Fund revenue. If the progress of these failures or malfunctions could be predicted or monitored in advance, their maintenance could be appropriately scheduled and their impact on operations could be minimized.

ORNL Electrical Signature Analysis Technology Development: Since 1985, researchers at the Oak Ridge National Laboratory (ORNL) have developed and patented several novel signal conditioning and signature analysis methods that have exploited the intrinsic abilities of conventional electric motors and generators to act as transducers. By using simple nonintrusive sensors such as clamp-on current and voltage probes, these diagnostic techniques provide an improved means of detecting small, time-dependent load and speed variations generated anywhere within an electro-mechanical system and converting them into revealing "signatures" that can be used to detect equipment degradation and incipient failures.

These developments have been grouped under the general name of electrical signature analysis (ESA) and together provide a breakthrough in the ability to detect, analyze, and correct unwanted changes in process conditions or the presence of abnormalities in electro-mechanical equipment.

Electrical signature analysis techniques were developed initially as a means of remotely monitoring the performance and condition of motor-operated valves (MOVs) used in nuclear power plant safety-related systems. Since then, they have been successfully demonstrated on a large variety of consumer and industrial equipment such as air compressors and water pumps, residential air conditioning units and heat pumps, large chillers, fans of various types and designs, automobile alternators and helicopter generators, home appliances and tools, and other devices.

Typical diagnostic information provided by ESA is comparable to that provided by conventional vibration analysis in that both time waveform and frequency spectrum signatures may be produced. The primary benefit of ESA is that an extensive range of diagnostic information can be obtained from a single transducer that may be installed several hundred feet or more from the monitored device on its electrical lines supplying input power (e.g., to a motor) or carrying output power (e.g., from a generator). Thus, ESA is truly remote and nonintrusive.

ESA is one of several nonintrusive diagnostic technologies developed at ORNL. These and other technologies have been transferred to industry through several nonexclusive patent licenses with UT-Battelle, LLC, which manages ORNL for the U.S. Department of Energy.

Project Goal and Methodology

C-141 ESA Project Goal: The goal of this project is to apply systems analysis and predictive maintenance techniques based on the application of electrical signature analysis to forecast impending fuel pump failures to reduce the unavailability of the C-141 aircraft due to unplanned repair or replacement of the fuel booster pumps.

ORNL Project Methodology: To accomplish this goal, the Systems Engineering Office of the C-141 Product Support Division of Warner-Robins Air Logistics Center tasked ORNL with a research and development project in three phases. The first phase demonstrated the validity of electrical signature analysis to diagnose defects within C-141 electric fuel booster pumps. The second phase of the project tailored the ESA analysis diagnostics to the fuel booster pumps and demonstrated the field application of these techniques. The third phase of this project will complete the database accumulation of both types of fuel pumps and develop prototype hardware and software for Air Force field evaluation.

In Phase II of the project, recently concluded, activities included (1) construction of a horizontal flow fuel pump test facility, (2) testing and determination of the electrical signature characteristics of populations of surplus fuel pumps from the Aerospace Maintenance and Regeneration Center (AMARC) facility at Davis-Monthan Air Force Base and pumps returned to the OC-ALC fuel pump repair depot after reconditioning, (3) correlation of changes in the electrical signatures associated with specifically implanted defects, (4) examination of returned fuel pumps from OC-ALC to determine their modes of failure, (5) development of software to perform ESA, (6) acquisition of a database of specific signatures and their associated defects, (7) determination of how to integrate ESA into existing Air Force maintenance and data management systems, and (7) performing a field verification of the ESA systems on C-141 aircraft of the 445th Air Reserve Wing (ARW) at Wright-Patterson Air Force Base (WP-AFB).

C-141 Fuel Booster Pump Testing

Fuel Pump Test Facility Design Features: A horizontal flow fuel pump test facility was constructed at ORNL. Two test tanks (Figure 3) were procured, one for auxiliary pumps and one for main pumps. Process water-cooling was used to eliminate fuel overheating during testing. The tanks are 24-in. tall × 24-in. wide × 44-in. long and are designed to contain 110 gallons of fluid. The pumps are inserted through an 11-in. × 11-in. inspection port opening on the top of the tank.

Figure 3: *C-141 horizontal flow auxiliary and main fuel pump test facilities at ORNL.*

An instrument control panel was constructed to operate the horizontal fuel pump test facility. This panel has digital readouts of fuel temperature, fuel pump outlet pressure, and fuel flow rate. In addition, both the auxiliary and main fuel pump power controls were routed through circuit breakers exactly as those used on the actual aircraft, so that problems similar to those that occur on an aircraft could be simulated with this facility.

Fuel Booster Pump Forensics: A sample of pumps was acquired from AMARC and OC-ALC for testing at ORNL. A total of 95 auxiliary pumps and 23 main pumps from AMARC were examined for defects in their "as-received" state. Those that showed no external damage were tested electrically using a megohmeter and a Baker Instruments Model 6A motor surge tester. The results of the forensic examinations of the fuel booster pumps from AMARC are shown in Table 1.

OC-ALC provided ORNL with a sample of 50 C-141 Condition F auxiliary pumps and 42 C-141 Condition F main pumps. The results of the forensic examinations of the fuel booster pumps are shown in Table 1.

Table 1: *Forensic data for pump test population*

Description	AMARC pumps		OC-ALC Condition F pumps	
	Main pumps	Auxiliary pumps	Main pumps	Auxiliary pumps
No apparent mechanical fault		45		17
Internal phase short		15		5
Missing parts	1	16	1	2
Foreign object damage (FOD)		9	15	13
Will not fit scroll housing		4	23	11
Loose front bearing, but runs		3		
Phases shorted to case		1		
Open windings				1
Not tested	22	2	3	1
Total received	23	95	42	50

Fuel Pump Hydrodynamic Performance Measurement

OC-ALC Reconditioned Pumps: The hydrodynamic performance curves of 12 main and 9 auxiliary reconditioned pumps tested at OC-ALC are shown in Figures 4 and 5, respectively. As may be seen, six of the main and two of the auxiliary pumps failed the minimum pressure or flow requirements.

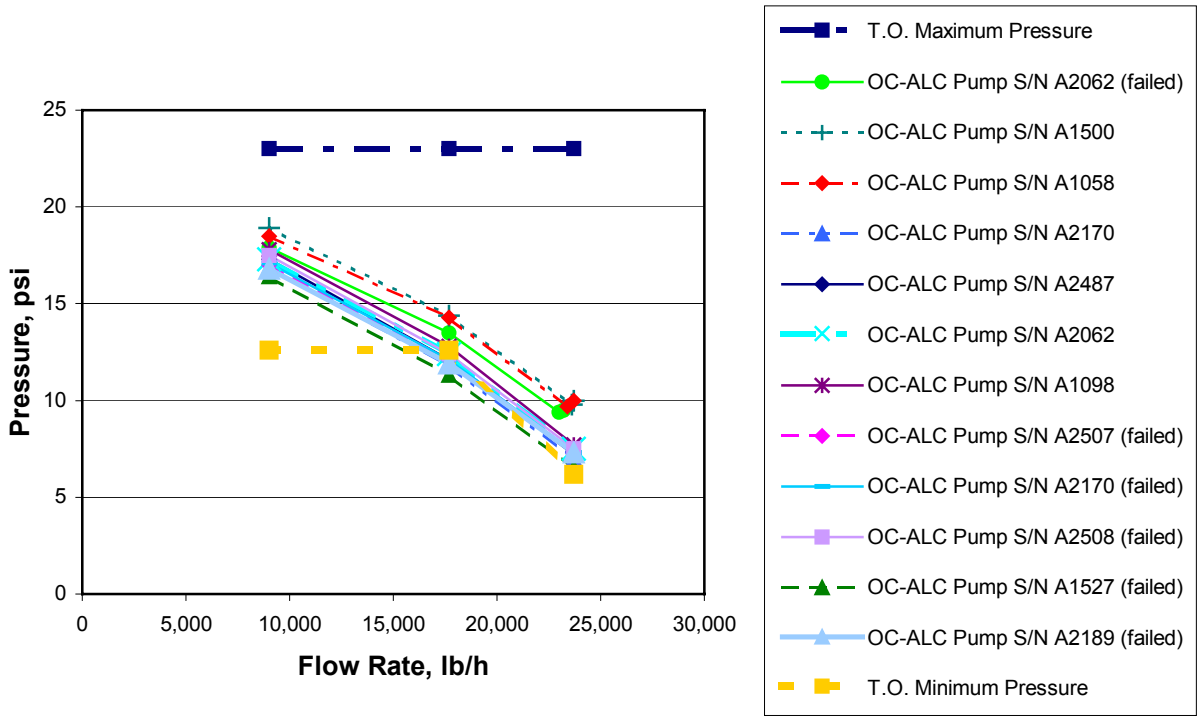

Figure 4: *OC-ALC reconditioned main pump hydrodynamic performance.*

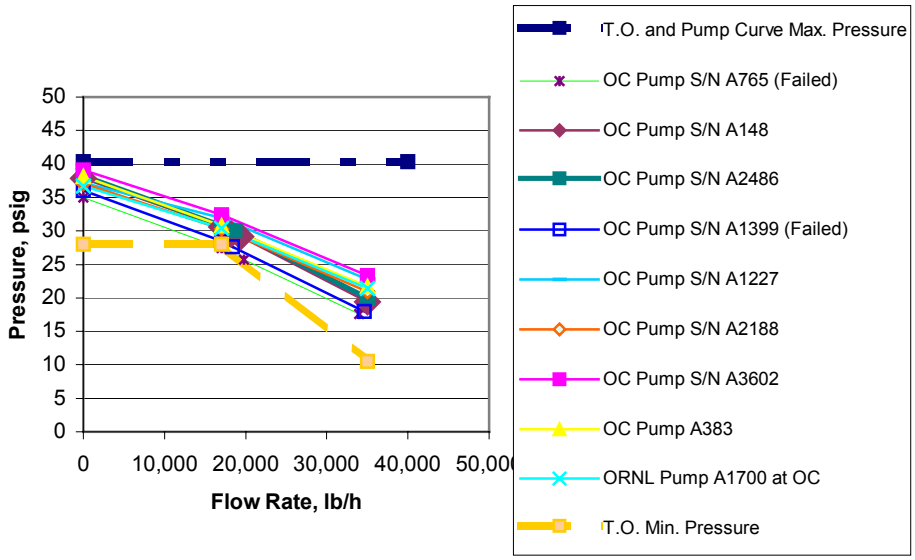

Figure 5: *OC-ALC reconditioned auxiliary pump hydrodynamic performance.*

AMARC Pumps Tested at ORNL: The hydrodynamic performance of 38 of the 46 AMARC pumps operable as received is shown in Figure 6. All of these pumps met the required minimum pressure and flow rate as prescribed by the Air Force technical operations manual.

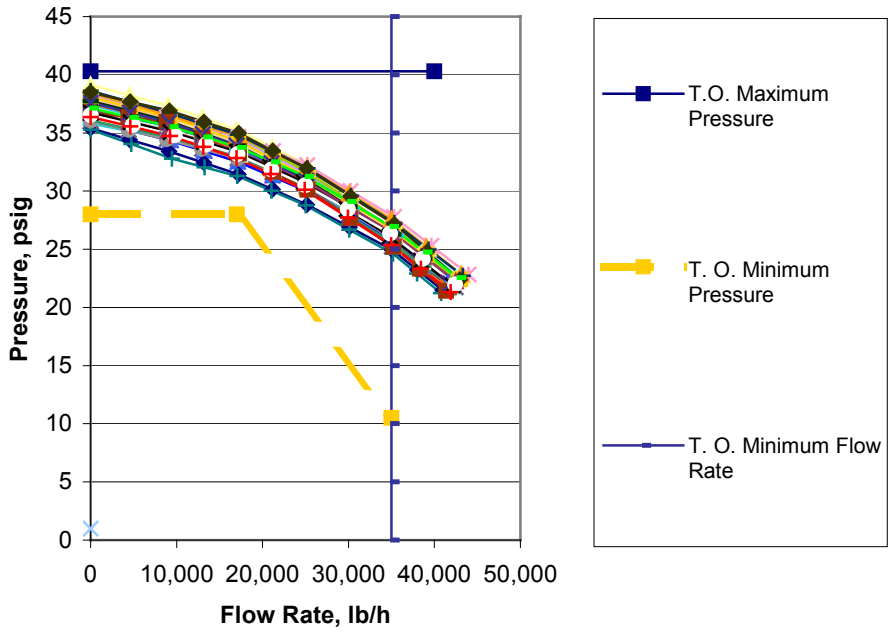

Figure 6: *Pump hydrodynamic performance of 38 as-received AMARC auxiliary pumps.*

To compare ESA field readings with laboratory readings, the effect of changes in phase voltage on an auxiliary pump's hydrodynamic performance is shown in Figure 7.

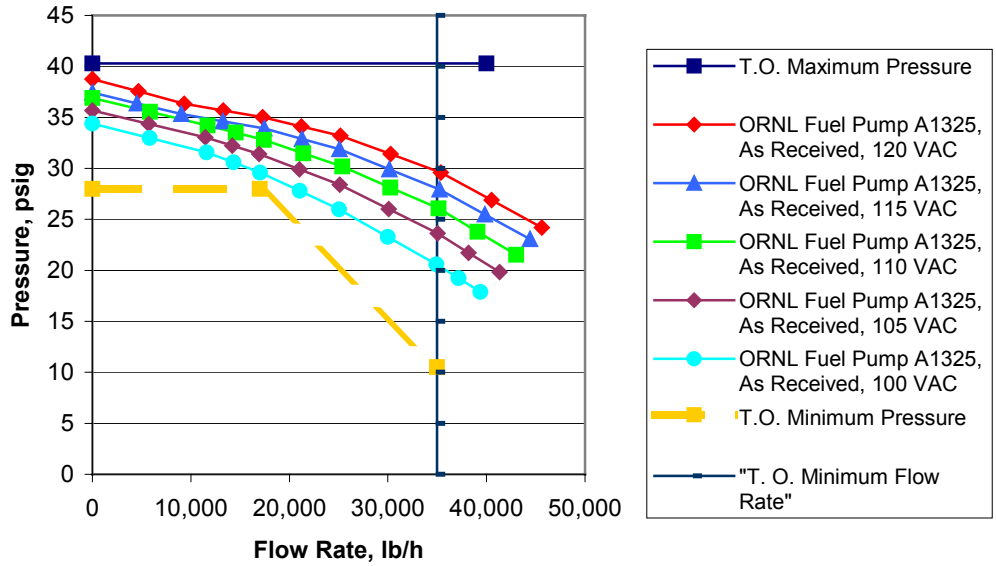

Figure 7: *Effect of changes in phase voltage on pump hydrodynamic performance, as compared to required performance.*

To determine the effect on hydrodynamic performance due to insertion of increased front bearing clearance (simulating wear), the hydrodynamic performance of five pumps was measured both as received and after inserting one level of increased front and rear bearing clearance. The typical hydrodynamic response of these pumps is illustrated by one of the pumps shown in Figure 8.

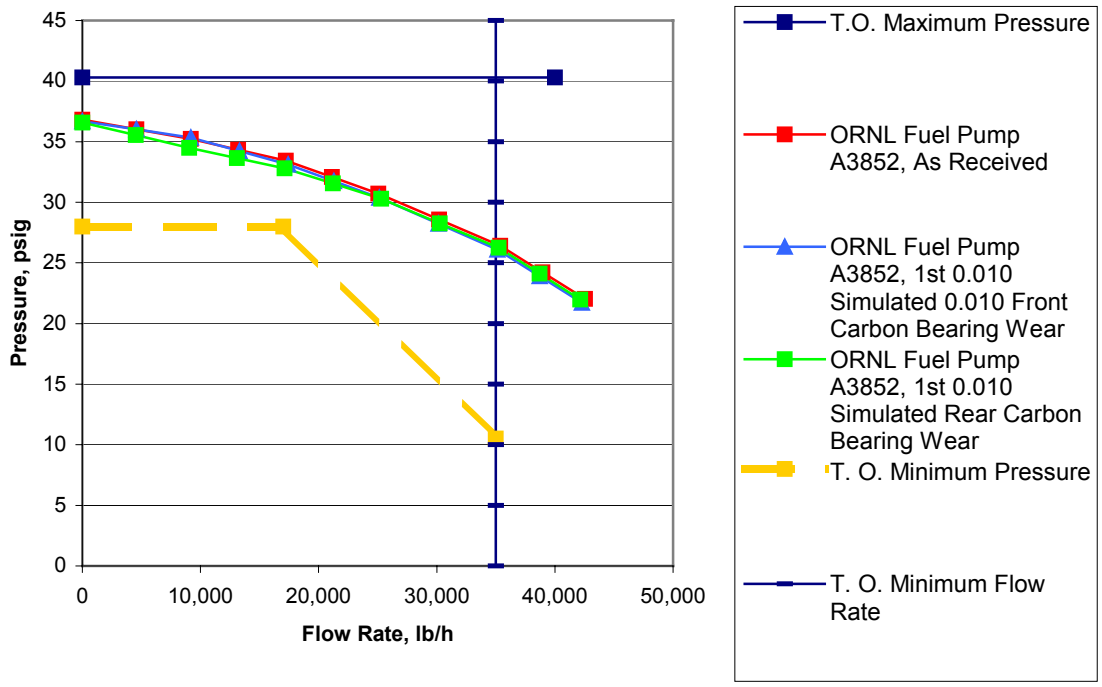

Figure 8: *Effect of changes in front and rear bearing clearance on auxiliary pump hydrodynamic performance.*

The pressure and flow characteristics of a pump are typical measures taken at OC-ALC. As can be seen from Figure 8, front and rear carbon bearing wear is not discernable using the standard test measurements.

Electrical Signature Analysis (ESA) Technology Description

Technical Basis and General Benefits of ESA: Electrical signature analysis (ESA) is a versatile and powerful technology that was invented at ORNL in 1985 and has since been successfully applied to a wide variety of military, industrial, and consumer equipment. ESA provides a breakthrough in the ability to detect and quantify undesirable process conditions and degradations in electro-mechanical equipment. Information provided by ESA is comparable to that provided by vibration monitoring systems, but since ESA only requires access to electrical lines rather than to the equipment itself, it can be used remotely and thus can often be used on otherwise inaccessible equipment that cannot be monitored by other methods. It does this by exploiting the intrinsic abilities of electric motors and generators to perform as *transducers*.

Figure 9 illustrates the basic principle behind ESA. Load and speed variations in electro-mechanical systems generally produce corresponding variations in motor current and/or generator voltage. ESA utilizes non-intrusive probes and specially developed signal processing methods to detect and analyze these small electrical perturbations and match them to their mechanical source. The resulting time and frequency signatures reflect loads, stresses, and wear throughout the system, thus providing the information necessary to assess the performance, condition, and operational readiness of the monitored equipment.

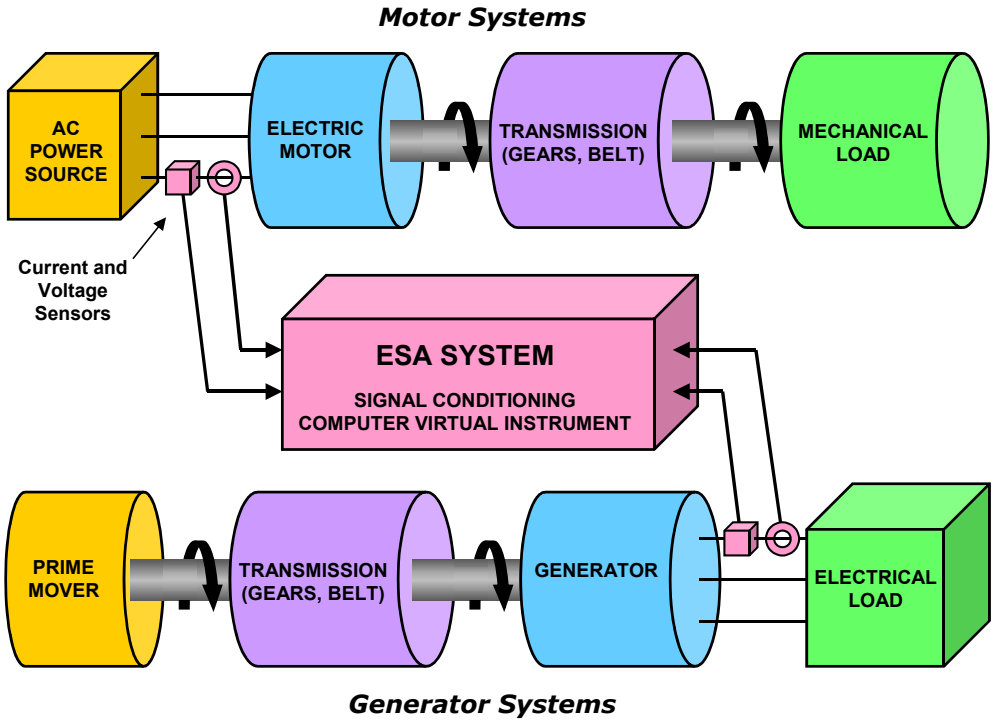

Figure 9: *Basic principle of ESA.*

Few available technologies can be so seamlessly integrated into existing maintenance programs. ESA provides the ability to pinpoint electrical and mechanical problems so that maintenance can be performed on an as-needed basis, thereby increasing equipment reliability and maintenance efficiency and minimizing unexpected downtime. The versatility of ESA as a condition monitoring technology is illustrated by the following examples.

Application Examples: At the request of the U. S. Nuclear Regulatory Commission, ORNL conducted a comprehensive assessment of motor-operated valves (MOVs) used in commercial nuclear power plants. A major objective of this study was to identify methods of monitoring the aging and service wear of MOVs in order to minimize unexpected failures that might lead to the unavailability of critical safety-related systems. In addition to evaluating the diagnostic information provided by several MOV-mounted sensors, considerable efforts were made to extract useful information from the motor's running current, since it could be acquired remotely (e.g., at the motor control center) and non-intrusively (using clamp-on current sensors). [1]

MOV motor current research led to the development of new techniques for using the MOV motor as a transducer for small time-dependent load and speed variations generated anywhere within the MOV and converting them into time-based and frequency-based signatures that reveal detailed diagnostic information at the subcomponent level as shown in Figure 10.

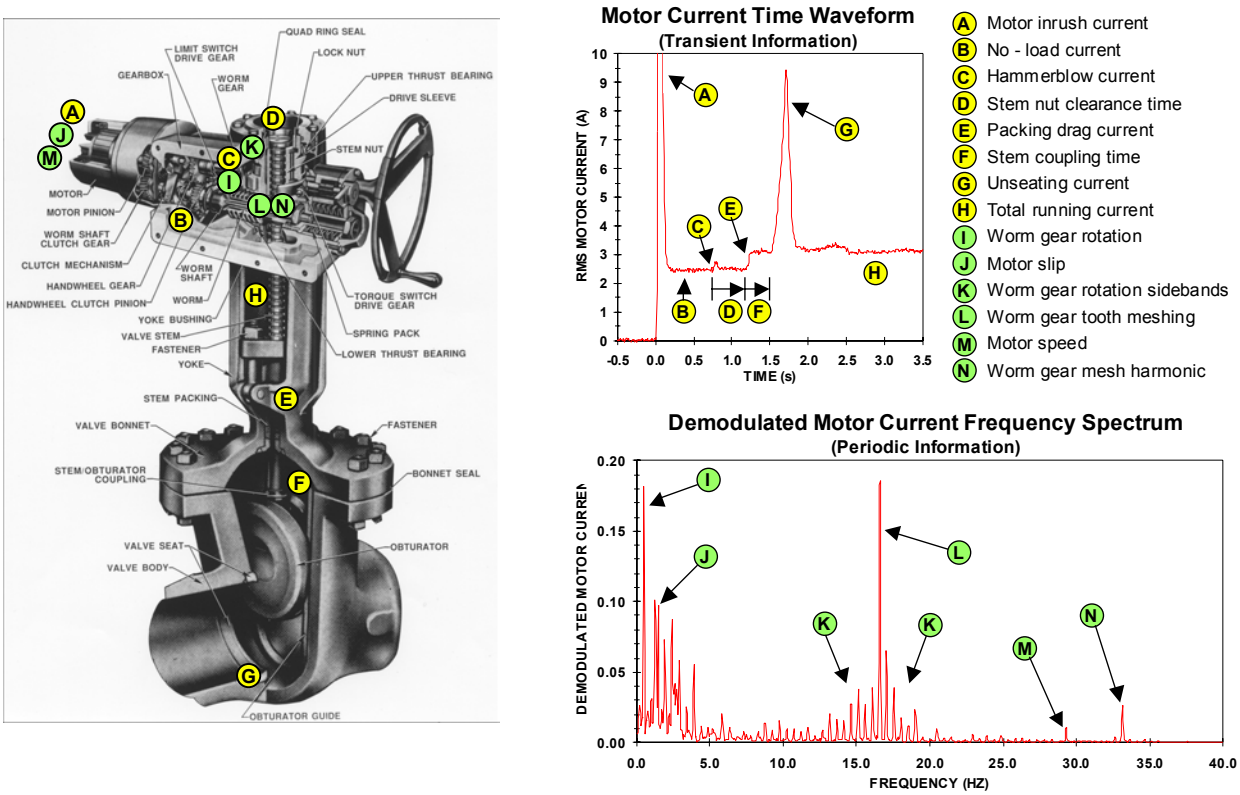

Figure 10: *Motor current time waveform and frequency spectrum for a motor-operated valve (left) showing multiple locations where degradation can be detected.*

It was discovered that by *demodulating* the raw motor current signal, the dominant power line frequency component was effectively removed, which revealed a considerable number of *modulator* frequencies that directly corresponded to mechanical load fluctuations that originated at separate locations throughout the MOV. [2] This ability to simultaneously monitor the operational behavior of many subcomponents from a single signal was unprecedented. For example, in a single motor current signal obtained over one hundred feet from the MOV, a bent valve stem, an over-tightened packing gland, a broken motor rotor bar, and even a single defective gear tooth on one of the many gears could now be detected *simultaneously*. This was possible because each of these defects produced a different signature feature that could be differentiated and identified.

The similarity between demodulated motor current signals and the signals from vibration transducers (e.g., accelerometers) cannot be ignored. Using a laboratory vacuum pump as an example, Figure 11 shows that the same frequency content can be present on both signals. The differences seen in the in peak magnitudes can be attributed to the differences in mechanical coupling between the source of the load perturbation and the transducer (accelerometer, electric motor) and further influenced by the sensitivity and frequency response characteristics of the transducer.

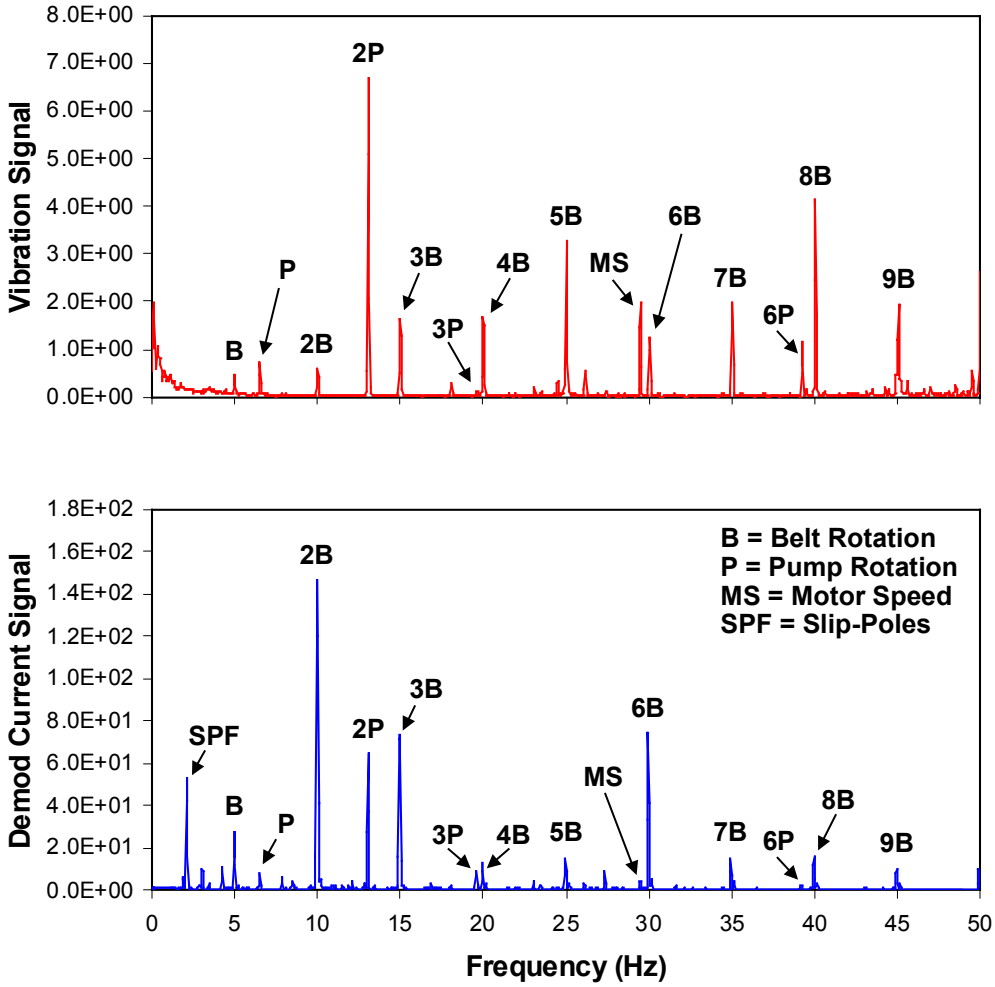

Figure 11: *Comparison between vibration (accelerometer) and demodulated motor current signals for a laboratory vacuum pump.*

One frequency component that is evident in the demodulated motor current signal and not in the vibration signal is the *slip-poles* frequency. This component is related to the motor shaft speed by the equation:

$$SPF = NP(SS-MS) \tag{1a}$$

where SPF = the slip-poles frequency, SS = the synchronous speed for the motor, and MS = the actual motor speed, all in Hz, and NP = the number of motor poles. Since the motor synchronous speed is equal to 2 times the power line frequency divided by the number of motor poles, equation (1a) may be rewritten as follows:

$$SPF = 2(LF)-NP(MS) \tag{1b}$$

where LF = power line frequency (e.g., 60 Hz or 50 Hz).

Since the variation in slip-poles frequency is several times that observed in motor speed, the slip-poles component provides a more sensitive indicator of subtle changes in motor speed that occur as a result of changing mechanical loads. Significant increases in the magnitude of the slip-poles peak have also been associated with motor rotor asymmetry, which can result from broken rotor bars.

Another component where ESA has been successfully applied is an aircraft integrated drive generator (IDG). IDG units provide power to aircraft (117/208 volts at 400 Hz) for passenger reading lights and galley microwave ovens. On certain aircraft, these units experience complete failure at an average rate of four per year; as many as ten have failed in one year. Failures are the result of seizure and destruction of scavenge, drive pump, and axial gears on the generator's main shaft. A gear set costs $17,000 and an entire IDG costs $250,000. Unfortunately, traditional recertification tests do not detect incipient gear failure. Thus, a new method for predicting gear failure could result in substantial savings for owners in replacement costs.

ORNL has demonstrated both on a test stand and on a commercial aircraft that ESA techniques provide the sensitivity to detect and characterize the condition of good and worn gears. The strength of ESA is that current and voltage probes are easy to attach, and that even at extremely low generator loads, ESA provides excellent sensitivity to the gear-related problems. Figure 12 shows that the magnitude of the scavenge pump gear mesh peak in the conditioned generator voltage spectrum can be used to differentiate a bad gear set from a good gear set.

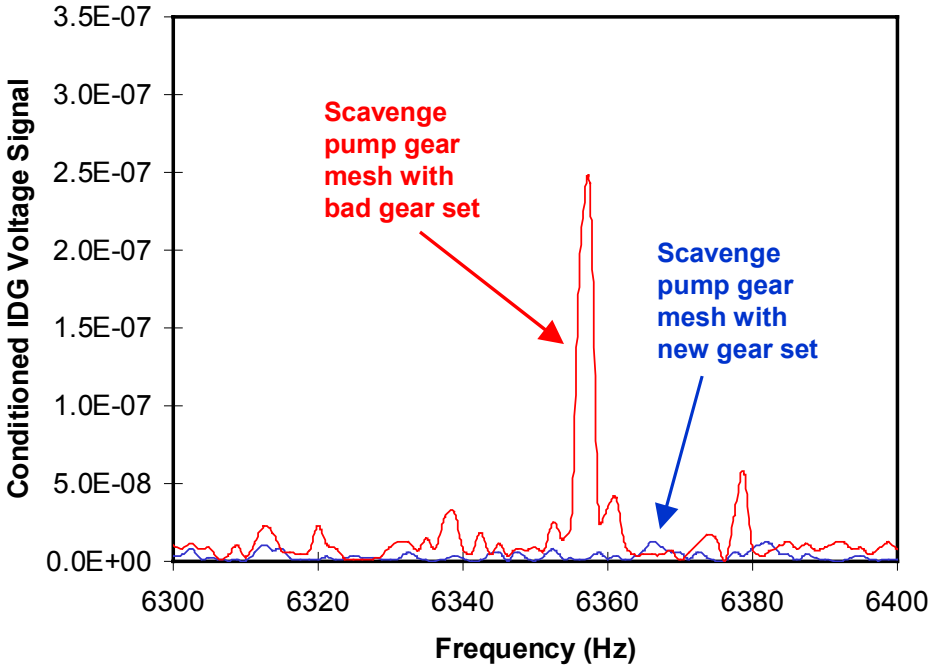

Figure 12: *Detecting a degraded gear set in an integrated drive generator using ESA.*

Trending ESA results over time provides the basis for equipment prognostics and for estimating equipment remaining life. Figure 13 shows how ESA was used to detect the load perturbations associated with the roller in a peristaltic pump. Each time one of the three rollers contacts and compresses a liquid-filled tube, the liquid is moved forward (pumped) which results in a momentary increase in motor running load. As the tube is repeatedly compressed and relaxed, it gradually looses its resiliency and ultimately can crack, which releases fluid and reduces or stops the flow of liquid to the intended location. These pumps are often used to re-circulate blood and to pump hazardous chemicals, so a tube rupture is highly undesirable.

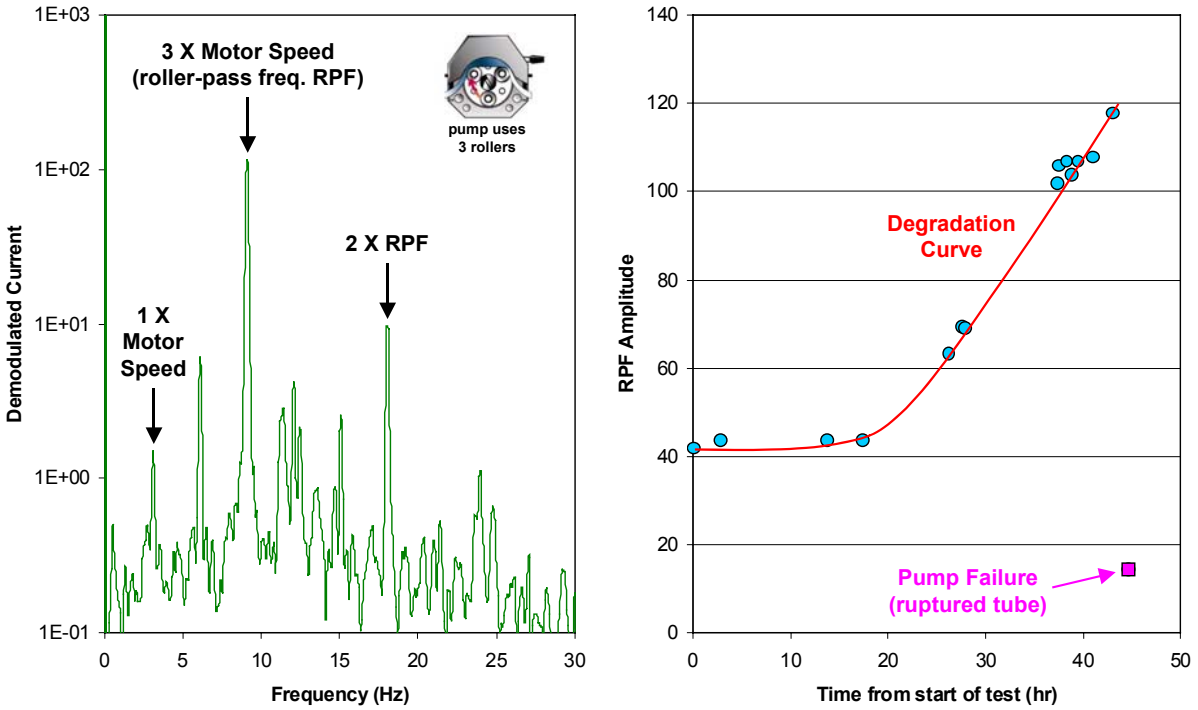

Figure 13: *Trending condition of a peristaltic pump with ESA.*

As shown in Figure 13, the roller-pass frequency (RPF) component was detectable in the demodulated motor current signal. By trending the magnitude of the RPF peak over time, a clear degradation curve is created and can now be used as the basis of estimating the remaining life of the tube. By moving or replacing the tube according to its condition, catastrophic failures can be minimized or prevented altogether.

ESA can detect unwanted changes in process conditions as well. In 1988, rotating stall was induced in a large axial-flow compressor at a major processing plant. This flow condition had been known to occur without warning on several occasions, and was a major cause of compressor blade fatigue damage and ultimate failure. Motor ammeter readings and equipment-mounted accelerometers had been tried unsuccessfully to detect this damaging aerodynamic condition. The interest in purposely inducing rotating stall in an operating process compressor was to determine if this condition could be detected with ESA.

ORNL installed a clamp-on current probe on the compressor motor ammeter loop in the facility control room, a location considerably remote from the compressor. Figure 14 compares demodulated motor current spectra both before and after rotating stall was induced. In both instances, frequency components were observed at the motor operating speed and at its slip-poles frequency (approximately 30 Hz and 1 Hz, respectively). When rotating stall was induced, new components at 13.5 Hz (fundamental rotation frequency) and 27 Hz (next harmonic) were immediately observed. These peaks remained in the demodulated motor current spectrum until the compressor was allowed to return to normal operation.

This test demonstrated that the motor was a superior transducer for detecting rotating stall. As a result, several motor-current-based alarm systems were subsequently installed at the plant.

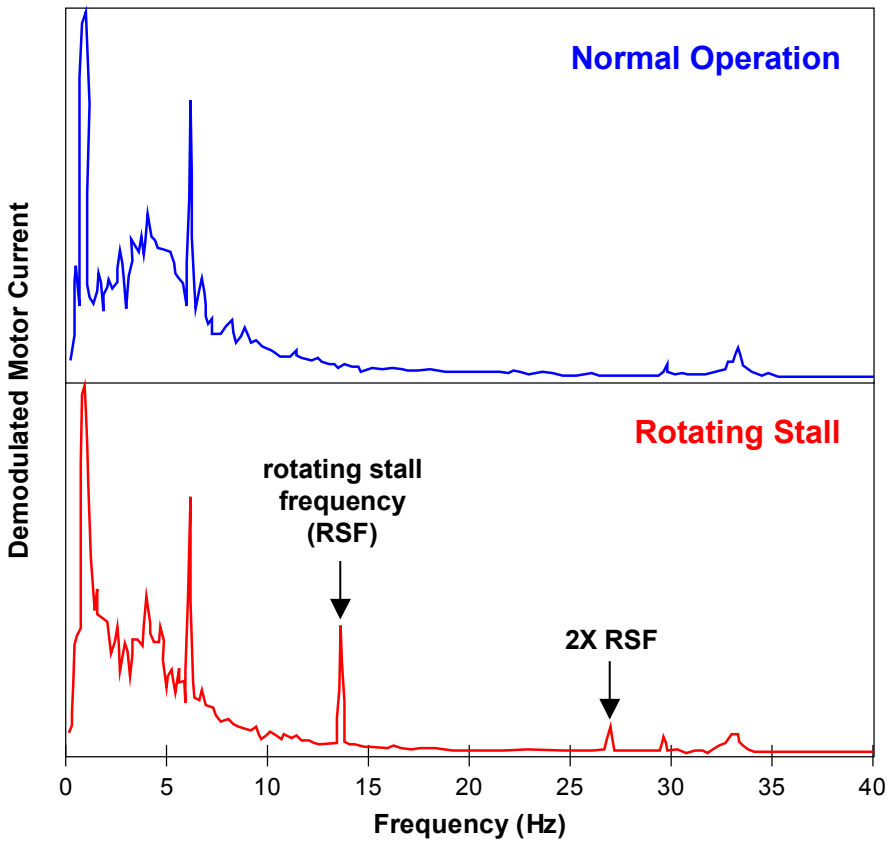

Figure 14: *Demodulated motor current spectra of a large axial-flow compressor demonstrating the ability of ESA to detect rotating stall.*

The operability and health of aircraft mechanical components can also be monitored non-intrusively by analyzing the voltage output from an electrical generator onboard the aircraft. For a turbine-driven rotor aircraft, available generators may include the aircraft systems' power-producing starter/generator and tachometer generators used to monitor turbine and rotor shaft speeds. To investigate this application of ESA, generator voltage signals were acquired on a Bell Jet Ranger helicopter while the helicopter was operated on the ground but "light on the skids." Figure 15 shows the helicopter in a "staged" condition, rather than an actual ESA test.

Also shown in this figure is a representative waveform from the rotor tachometer generator (RTG) and its corresponding frequency spectrum. In addition to the large fundamental frequency indicative of the rotor's speed, several harmonics are shown. The relative magnitude of these harmonics (i.e., harmonic distortion) was observed to change with rotor unbalance, which was induced by installing additional mass near the end of one rotor blade. Although a detailed data analysis is beyond the scope of this paper, a strong correlation was discovered between rotor unbalance and harmonic distortion of the RTG signal (see Figure 15).

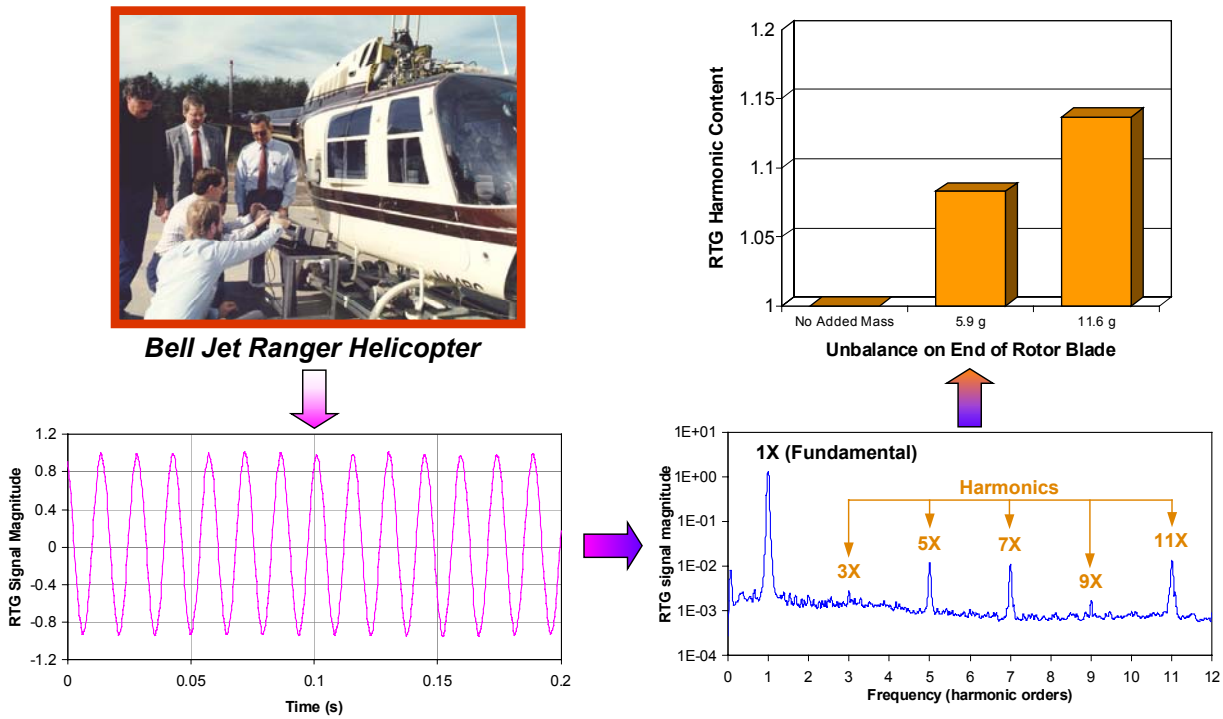

Figure 15: *Detection of helicopter rotor unbalance using ESA of the rotor tachometer generator (RTG) voltage output.*

The aircraft's power-producing starter generator was also seen to behave as a sensitive transducer whose signal was influenced by mechanical loads throughout the helicopter's complex gear train. The primary dc voltage provided by the generator was seen to coincide with a smaller, but inherently useful, ac signal component as well. The ac component was seen to contain discrete frequency elements that directly corresponded to several known gear meshings within the helicopter's transmission. These correlations demonstrate that the transducing abilities of onboard aircraft generators far exceed their recognized functions (e.g., speed monitoring and battery charging). [3]

In addition to the examples provided in this paper, ESA has been successfully applied to many other electro-mechanical devices. These devices include: Army portable power generator-sets, Navy fire and seawater pumps, a prototype Army ammunition delivery system, a NASA propellant control valve, fuel injectors and solenoid valves, heat pump and air conditioning systems, nylon spinning machines, large blowers and fans, coal pulverizers, variable-speed motors, multi-axis industrial cutting machines, electric vehicle motors and alternators, consumer power tools and appliances, and other devices.

The remainder of this paper will focus on the recent application and development of ESA as a condition monitoring technology for electric fuel booster pumps used on the C-141 aircraft. The reader is advised that this is an ongoing project and that additional developments may have occurred after this paper was prepared.

Application of ESA to C-141 Fuel Pumps for Detecting Fuel Pump Failure Modes

The importance of an ESA-based monitoring method for C-141 fuel pumps is clear when one examines the C-141. Each aircraft utilizes a total of twenty fuel pumps, dispersed symmetrically ten per wing. As illustrated in Figure 16, each wing contains five fuel tanks—two main tanks, two auxiliary tanks and one ER tank—with two pumps (a primary and a secondary pump) handling each fuel tank.

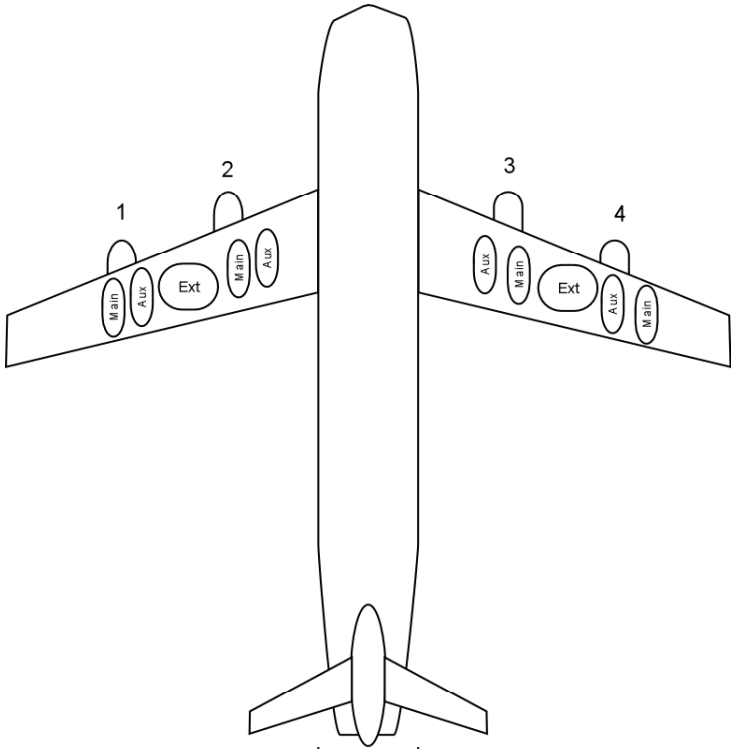

Figure 16: *C-141 engine and fuel tank locations.*

C-141 fuel pumps are installed inside their fuel tanks and are intended to operate completely submerged in fuel. After installation, they are inaccessible for monitoring by conventional vibration instrumentation. ESA provides a unique means of monitoring fuel pump operational condition without requiring that anything be installed on the pumps themselves, and only requires access to electrical leads. Figure 17 shows that C-141 fuel pump leads can be easily accessed under the wings and inside the fuselage. At these locations, fuel pump current signals are obtained using clamp-on current probes that can be installed on live conductors without special precautions and without interrupting any aircraft operations. The current probe output leads are connected to data acquisition equipment, which only needs to operate for a few seconds. The clamp-on current probes are then removed, leaving the aircraft's wiring as it was found before data were acquired.

To provide a consistent platform for obtaining and analyzing fuel pump electric current data, a first-generation portable system was developed early in the project. This system, shown in Figure 18, includes clamp-on probes for sensing current in all three pump electrical phases plus neutral, signal conditioning electronics for signal buffering and anti-alias filtering, and a portable computer running several virtual instruments (VIs) that are based on LabVIEW™, a commercially-available software development system. Presently, a "suitcase-style" ESA-based diagnostic system is under development. This system is expected to serve as a platform for other potential aircraft diagnostic applications such as flight control surface drive actuators, landing gear bay door actuators, integrated drive generators, etc. At the end of the project, two prototype ESA systems will be delivered to the Air Force for their use on C-141 fuel pumps.

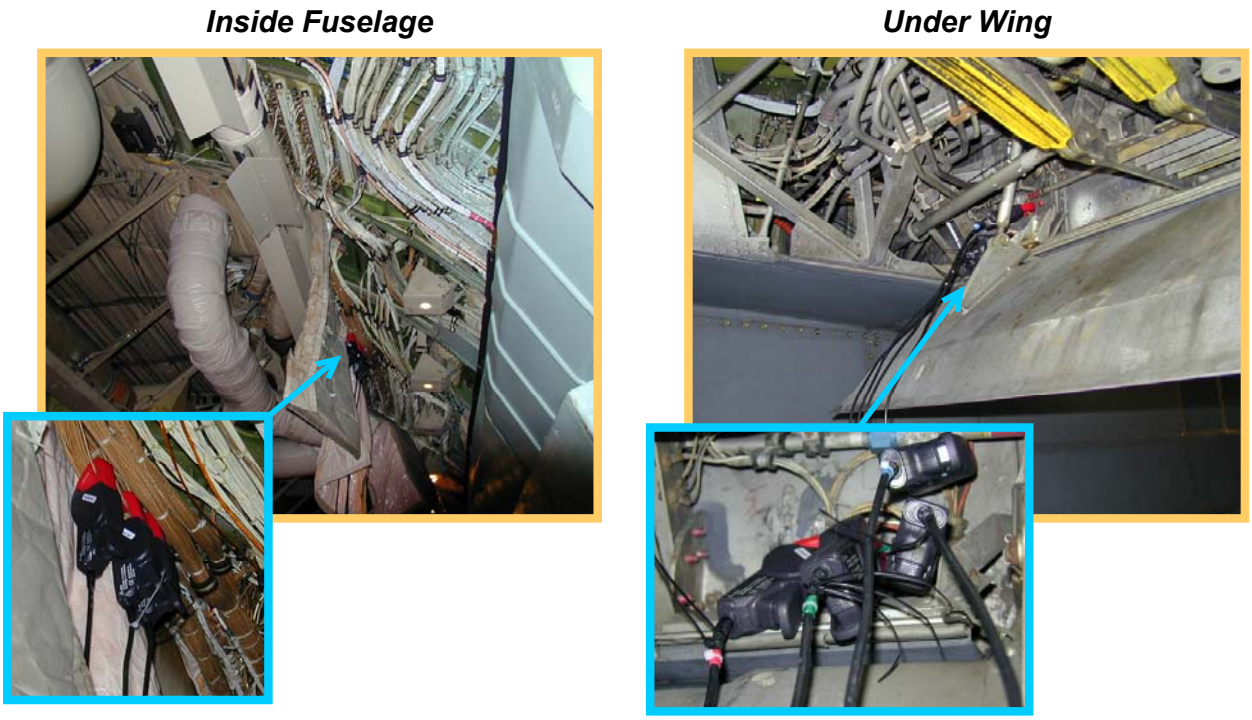

Figure 17: *C-141 fuel pump motor current leads are easily accessible inside the fuselage (left) and under the wing (right).*

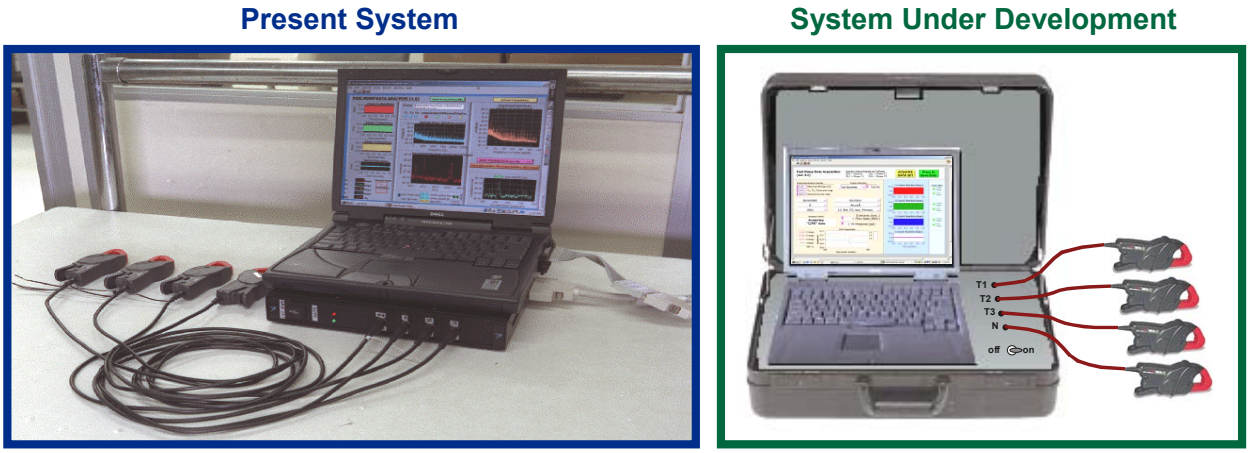

Figure 18: *Portable ESA system (left) presently being used, and a concept of a "suitcase-style" ESA-based system (right) under development.*

Since the major objective of this project is the development of an ESA-based fuel booster pump condition monitor for the C-141 aircraft, it was felt that this should be accomplished through a progression of activities outlined by the flowchart shown in Figure 19. The flowchart identifies several sequential steps that are being taken to develop the tools and knowledge that are necessary for a prototype condition monitoring system.

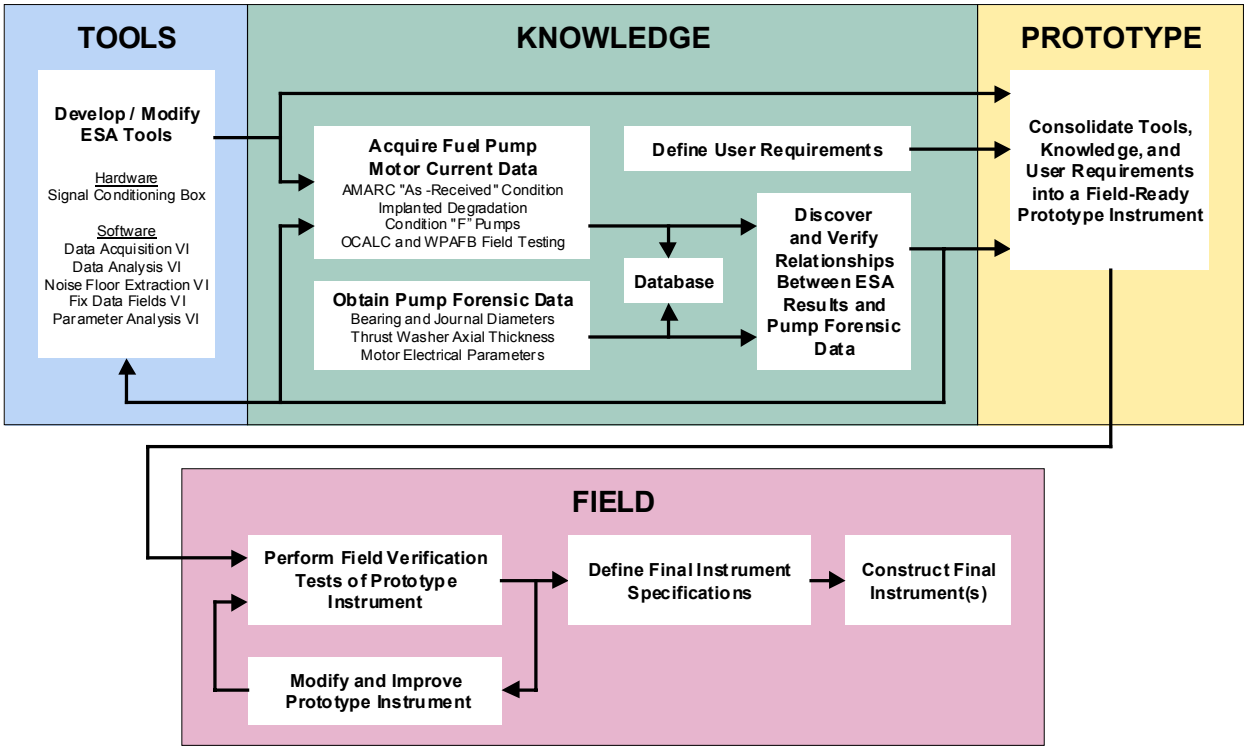

Figure 19: *Research and development plan.*

During this project, C-141 fuel booster pump hydrodynamic performance and electrical signature data have been obtained from three locations: OC-ALC (pumps in test stands), WP-AFB (pumps installed on aircraft), and a test loop constructed at ORNL. While considerable main and auxiliary pump data have been acquired thus far from these sites, the data analysis efforts have focused almost exclusively on auxiliary pumps.

Figure 20 shows a typical auxiliary fuel pump motor current waveform. It is a rather normal-looking 400 Hz sinusoid that reveals very little of what is contained in it.

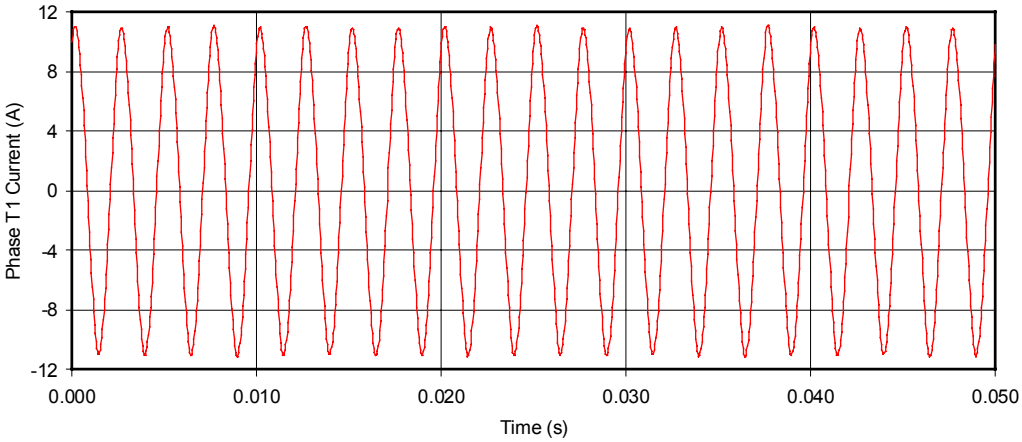

Figure 20: *Auxiliary fuel pump motor current waveform.*

When this waveform is viewed in the frequency domain, the complex structure suggesting that diagnostic information may be present is revealed. Figure 21 shows the large number of frequency components that are present in a typical auxiliary fuel pump motor current spectrum. When pump flow rate is changed, these peaks move in a manner that confirms their sensitivity to flow rate and thus enhances their potential diagnostic value.

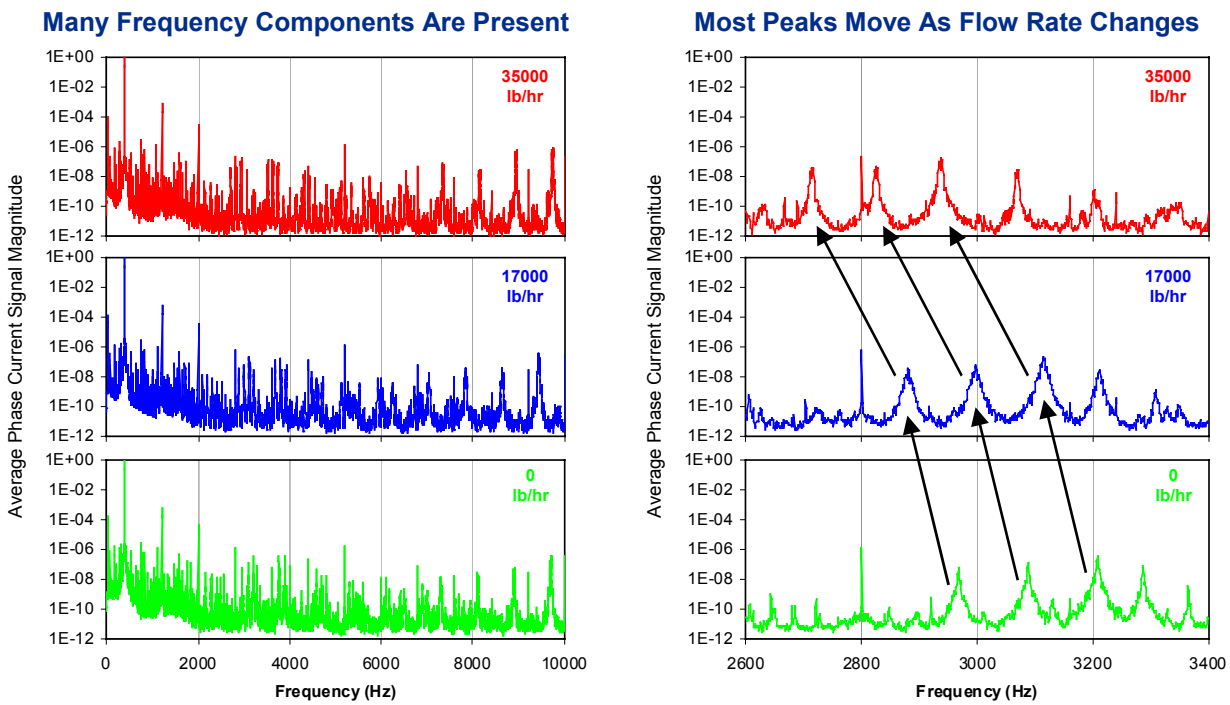

Figure 21: *Auxiliary fuel pump "raw" motor current spectra under three different flow rates.*

The complexity of the motor current spectrum makes it difficult to analyze in its "raw" state. One reason for the complexity is that a single periodic perturbation, or *modulation* to the 400 Hz line frequency will result in a pair of peaks based on the frequencies of the line frequency and modulation. A way to simplify the spectral contents is to *demodulate* the spectrum using either analog or digital (e.g., via software) methods. The virtual instrument (VI) used for analyzing the fuel pump motor current signals employs a digital amplitude demodulation scheme, which results in spectral sideband consolidation and effectively simplifies the motor current spectrum for analysis. After demodulation, key frequency components were discovered at the fundamental speed and slip-poles frequency of the auxiliary fuel pump motor as shown in Figure 22.

It was found that for most auxiliary fuel pumps, motor speed can be determined directly from the demodulated motor current spectrum with a fairly high confidence. The frequency of all other spectral peaks may then be represented in *orders* of running speed. Frequency components having an integer order are *harmonics* of motor speed. Their harmonic number then provides a clue as to their origin, when key design details of the fuel pump are taken into consideration. For example, Figure 23 shows that a frequency component is present in the demodulated spectrum at 24-times (24x) running speed. Other peaks shown in this figure are at 28x, 29x, and 30x. The figure lists major frequency components (ESA parameters) that are found in the auxiliary fuel pump motor current spectrum and their possible relationship to pump and motor design.

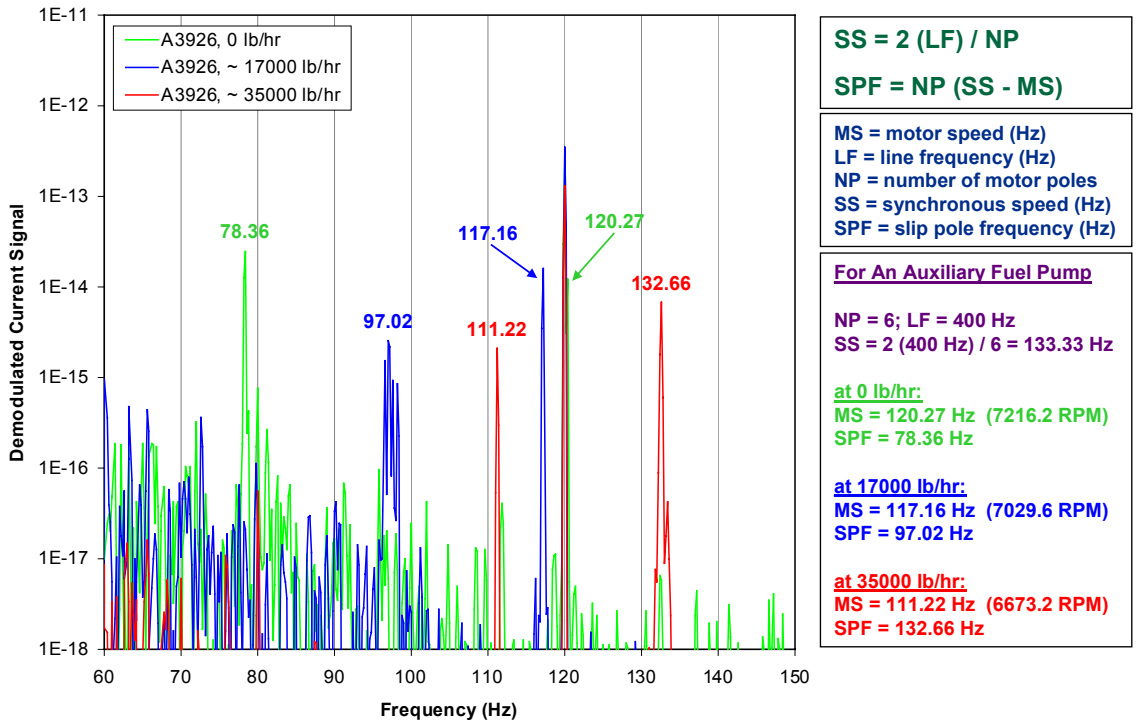

Figure 22: *Demodulated motor current spectra from an auxiliary fuel pump operated at three flow rates showing motor speed-related peaks.*

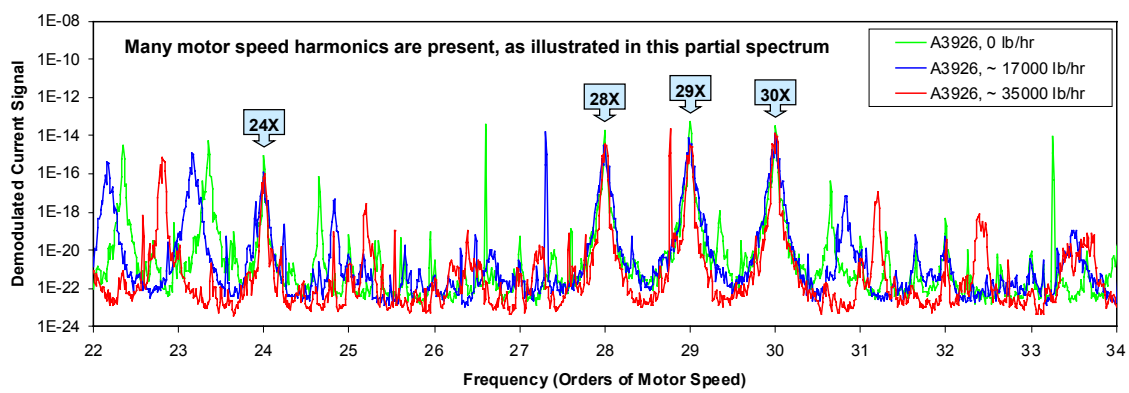

ESA Parameter	Relationship With Auxiliary Pump And Motor Design
1xMS, 2xMS	Fundamental and second harmonic of motor speed.
motor slip-poles	The magnitude of the slip-poles peak increases with motor rotor bar degradation.
4xMS	The pump has 4 impeller vanes.
6xMS, 12xMS, 18xMS, 24xMS, 30xMS, 36xMS	These harmonics represent multiples of 6x (the motor has 6 poles) or possibly a center frequency at 18x (the motor has 18 stator slots) that is modulated by 6x.
28xMS, 56xMS	The motor has 28 rotor bars. 56 = 2 x 28
54xMS	54 = 3 x 18, where 3 = number of motor phases, 18 = number of motor stator slots.
84xMS	84 = 3 x 28, where 3 = number of motor phases, 28 = number of motor rotor bars.

Figure 23: *Demodulated motor current spectra from an auxiliary fuel pump, plotted in orders of motor speed.*

In addition to frequency spectrum analysis, fuel pump hydrodynamic performance curves can characterize the relationships that exist between measurable parameters, such as flow rate, discharge pressure, motor running current, and motor speed. Figure 24 illustrates typical relationships between these parameters for an auxiliary fuel pump tested in the ORNL test facility.

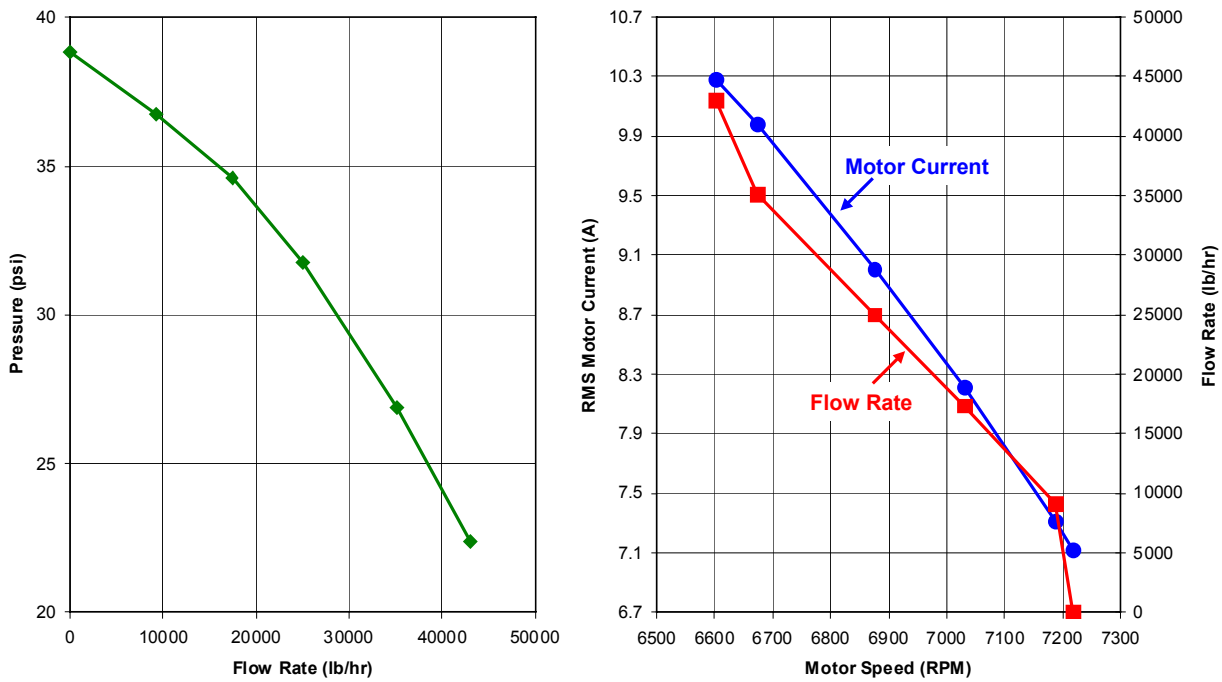

Figure 24: *Relationships between several auxiliary fuel pump parameters.*

The relationships between flow rate, motor current and motor speed are also well illustrated by a test that was carried out at WP-AFB on an auxiliary fuel pump that was transferring fuel from the engine three primary fuel tank to the extended range tank in the same wing. Figure 25 shows that before the fuel transfer began, the auxiliary fuel pump was operated at deadhead conditions (zero flow), where the pump's running current was approximately 7.6 amps. During the fuel transfer, the running current rose to approximately 11 amps. After a little more than two minutes into the transfer, the motor current precipitously dropped to less than 6 amps, and eventually the pump was shut off after the running current had dropped to nearly 4 amps. As illustrated by the figure, increasing flow rate pushes the pump motor to work harder, which results in the motor slowing down and drawing more current. Conversely, as the pump apparently runs dry, the motor speeds up and the current drops to levels below that which is observed at zero flow. This indicates that even at deadhead conditions, the fuel pump sees more mechanical load than when the pump's impeller no longer feels the drag of the surrounding fuel. The relationship between motor current, speed, and running load that is observed at this *macro* level is also seen at a much smaller *micro* level when much smaller changes in running load occur.

The real value of ESA is as a non-intrusive technology for detecting these small-effect degradations in electro-mechanical components and systems. Degradations can often be detected as a change in frequency or magnitude of a single spectral component, which may easily represent less than one percent of the entire motor current signal. Changes in motor current at these levels can never be detected in the overall RMS motor current magnitudes, but require detailed spectrum analysis of raw or demodulated signals.

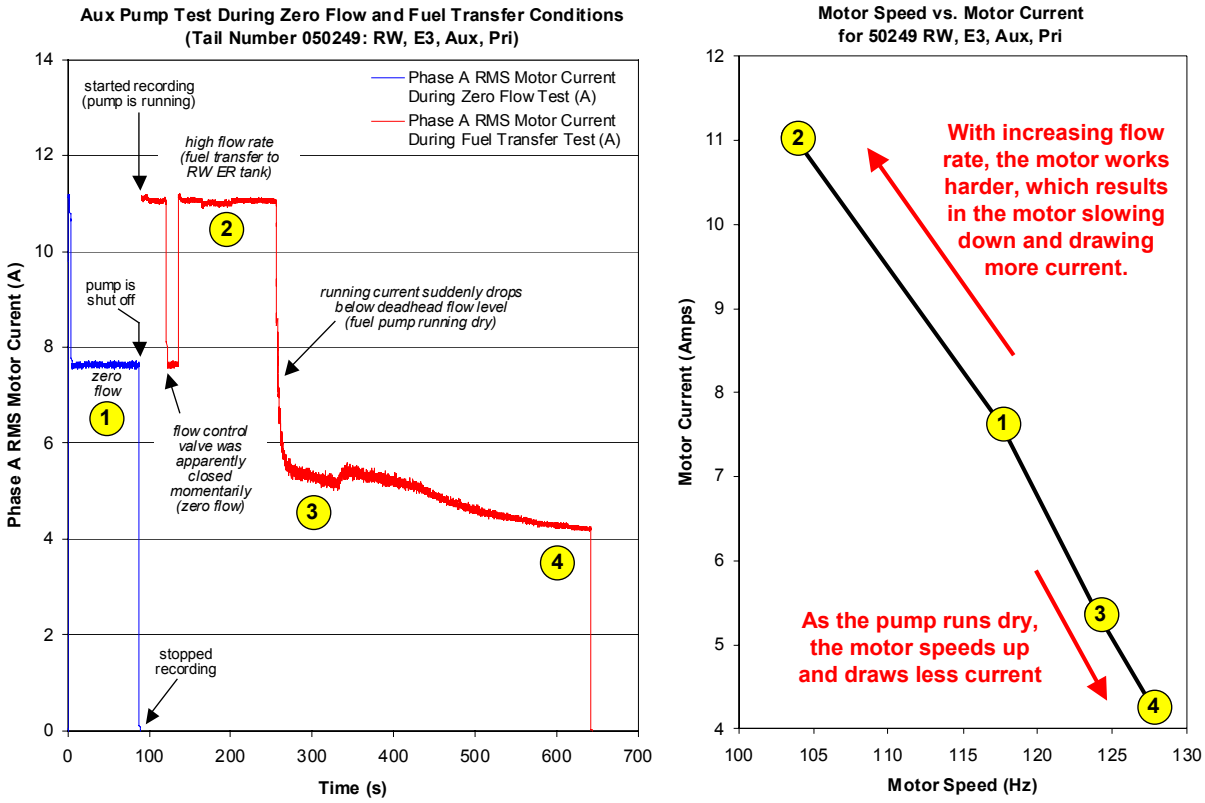

Figure 25: *Fuel transfer test performed on an aircraft at WP-AFB.*

In order to develop ESA as a fuel pump diagnostic technology, it was desired to test fuel pumps in both typical operational condition and in degraded condition, where the type and level of the degradation were known. This work is presently being done at ORNL, using a fuel pump test facility that is capable of testing both main and auxiliary fuel pumps. Before these tests could begin, the types of degradation common to C-141 fuel pumps were determined from several discussions with maintenance personnel. The degraded conditions observed in C-141 fuel booster pumps include:

- foreign object damage (FOD),
- axial thrust washer wear,
- impeller / shroud blow by,
- motor electrical degradation,
- impeller imbalance due to nicks or abrasion,
- front carbon bearing or journal wear, and
- rear carbon bearing or journal wear.

From this list, bearing wear was selected as the first degradation to study. Ninety-five auxiliary fuel pumps were obtained from AMARC. The fuel pumps were disassembled and carefully inspected prior to flow facility testing. An inspection of the auxiliary pumps from AMARC showed that front bearing wear is more common than rear bearing wear, since the clearance between the front carbon bearing and the front journal was in almost all cases greater than the rear bearing / journal clearance. This is illustrated in Figure 26.

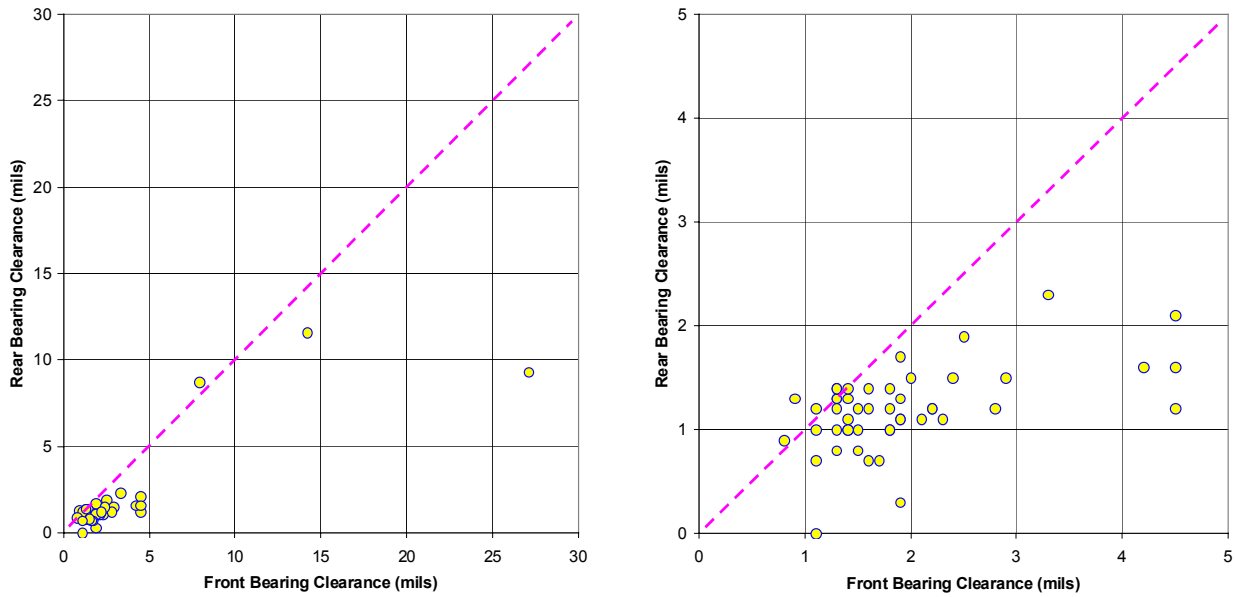

Figure 26: *Front and rear bearing clearances of auxiliary fuel pumps from AMARC.*

Based on this evidence, it was decided to focus on front bearing degradation. To determine if ESA methods could detect front bearing wear, five auxiliary fuel pumps were tested in "as-received" condition and after increasing the front bearing internal diameter about 0.010-inch. An examination of the hydrodynamic performance curves for the five pumps showed that they did not provide a reliable means of detecting the additional bearing wear. Performance curves for two of these pumps are shown in Figure 27.

Efforts were then focused on developing an ESA technique that could quickly detect bearing wear in fuel pumps that are installed in flow test loops and in C-141 aircraft. An ESA-based method that could detect fuel pump bearing wear at deadhead (zero flow) conditions would be particularly beneficial since:

- An ESA-based method would only require access to the motor power leads.
- Zero flow conditions are easy to establish on an aircraft while on the ground.
- Although a significant fuel pump flow rate can be established (from tank to tank transfers), zero flow testing is less intrusive.
- An ESA diagnostic method that can be used at zero flow is more "robust" than a method that is sensitive to flow-rate variations.

After considerable study, it was determined that the best indicator of front bearing wear in the motor current spectrum was not a specific frequency peak, but was the base, or floor of the spectrum. The noise floor of the demodulated motor current spectrum at deadhead conditions was observed to increase in all five pumps having the degraded front bearings. Figure 28 graphically explains what is referred to as the noise floor. This figure also shows that the increase in the noise floor was especially prominent within a range bounded by 20-times motor speed and 40-times motor speed (20x–40x). Within the 20x–40x range, the average noise floor increased over two orders of magnitude (greater than 100 times) as a direct result of the additional front bearing wear.

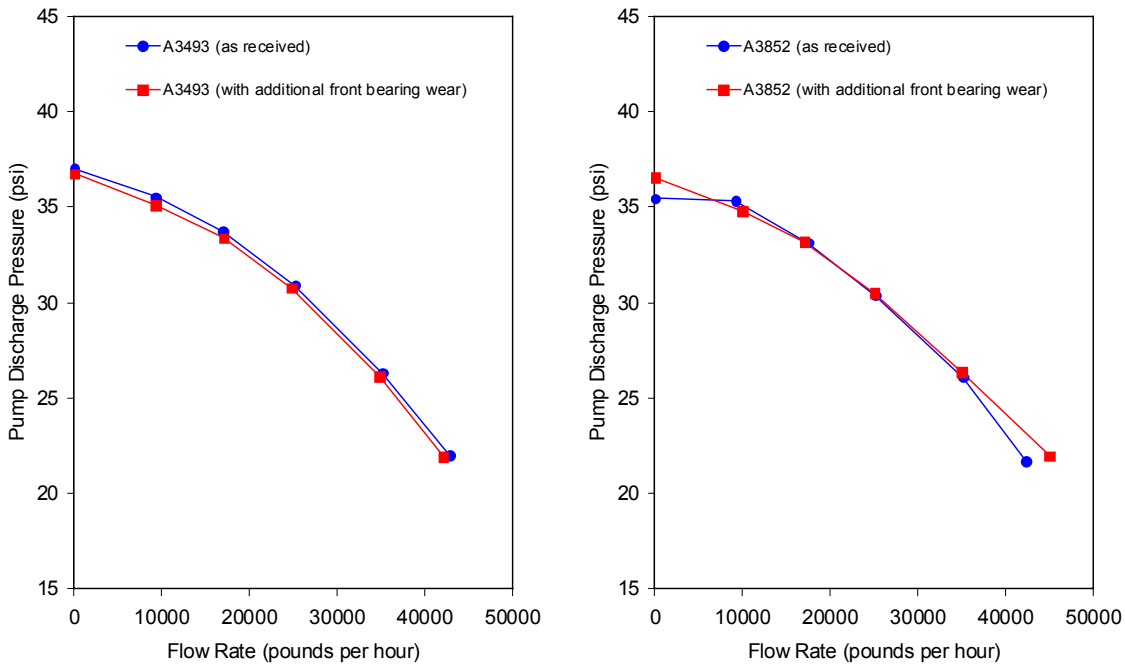

Figure 27: *Hydrodynamic performance curves for two auxiliary fuel pumps before and after the introduction of 0.010-inches of additional wear on the front bearing.*

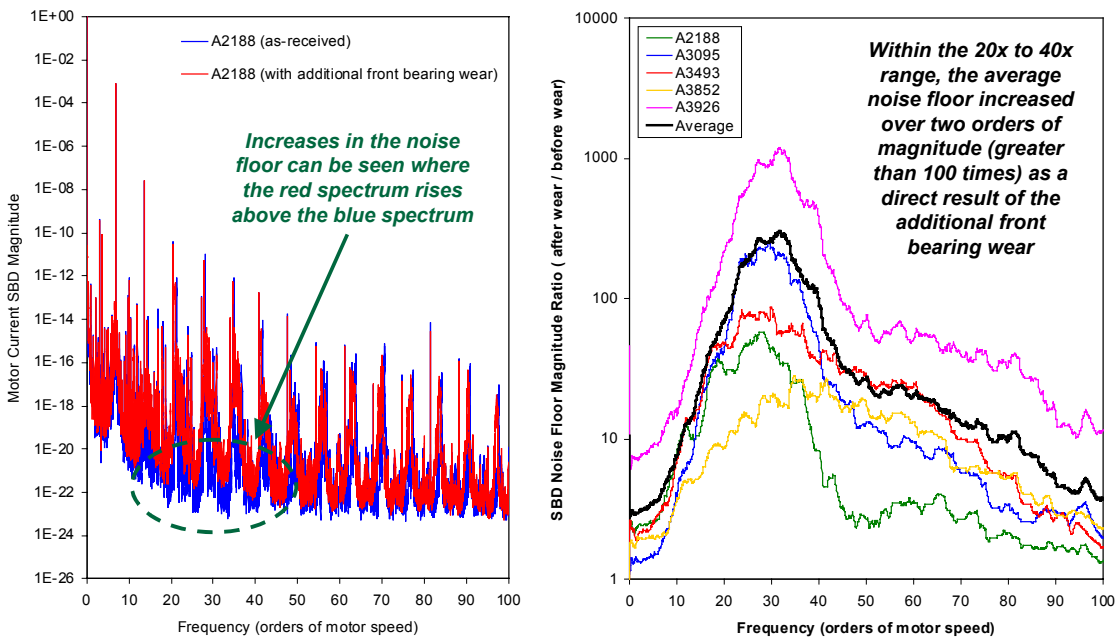

Figure 28: *Change in the noise floor of the demodulated motor current spectrum as a result of increased front bearing wear.*

Once this discovery was made, the 20x–40x noise floor magnitudes were plotted for all tested auxiliary pumps from AMARC where the bearing dimensions were known. Figure 29 illustrates that there is a strong relationship between front bearing wear and the 20x–40x noise floor measurement, thus making it a suitable ESA method for detection of this problem.

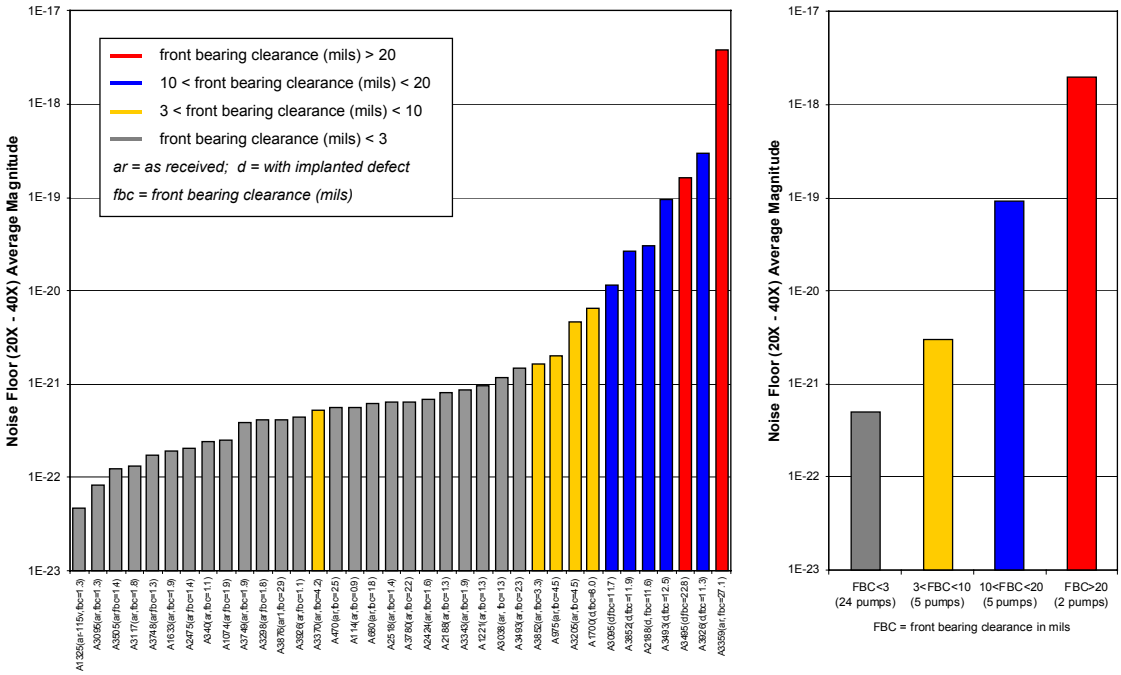

Figure 29: *Relationship between auxiliary pump front bearing clearance (FBC) and the 20x–40x noise floor magnitudes from the demodulated motor current spectra at zero flow.*

When all other auxiliary pumps are added to this plot, a few pumps that were tested at WP-AFB and at OC-ALC were seen to exhibit the high noise floor levels that are indicative of front bearing wear, although the front bearing clearances of these pumps are not known. These results are presented in Figure 30.

Since motor electrical degradation is also a concern, several measurements were made that might expose differences in condition between the motors used in the auxiliary fuel pumps that have been tested so far. Figure 31 shows the distribution in neutral current and current unbalance for all tested auxiliary pumps at zero flow. Several pumps having unusually high neutral current were also identified as having other problems (e.g., worn front bearings, failure to pass OC-ALC pressure-flow criteria). Several pumps tested on aircraft 60132 were also observed to have unusually high current unbalance. Only one known motor electrical problem was present in this population: the internal phase short in AMARC pump A708 that was tested at Oak Ridge. This failure adversely affected both the neutral current and current unbalance measurements in an easily detectable way.

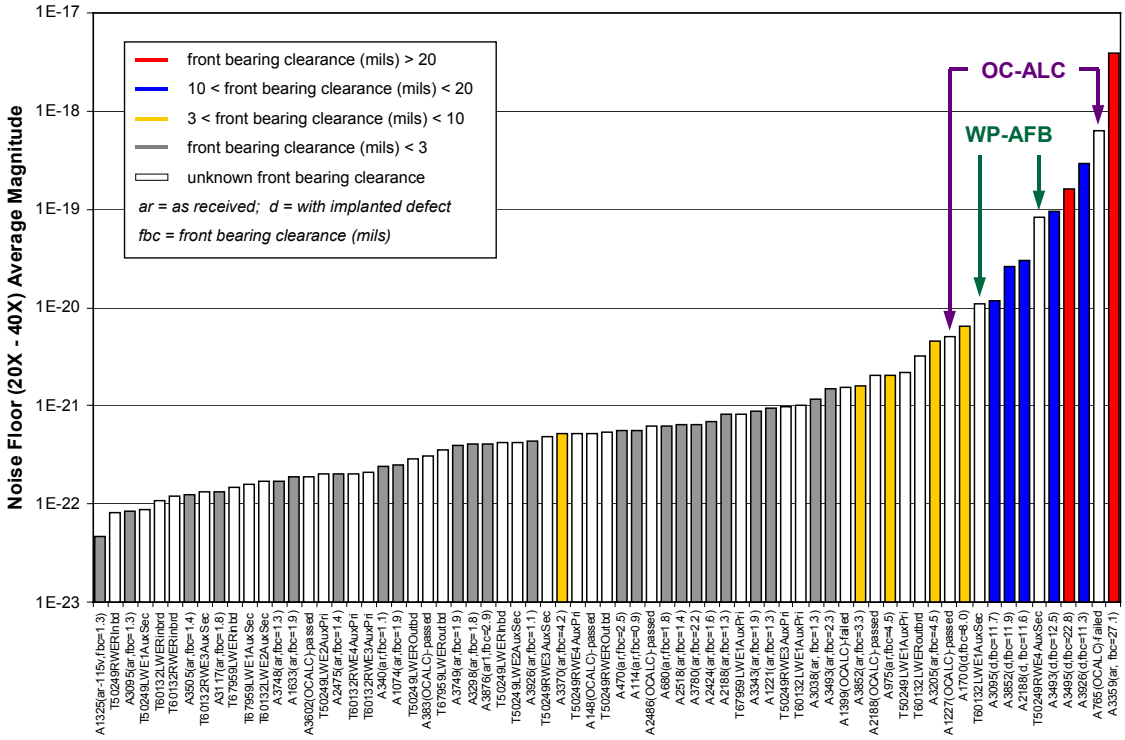

Figure 30: *Noise floor measurement (20x–40x) for all tested auxiliary fuel pumps tested at zero flow. Several pumps tested at WP-AFB and OC-ALC exhibit high levels that are indicative of front bearing wear, although this was not confirmed.*

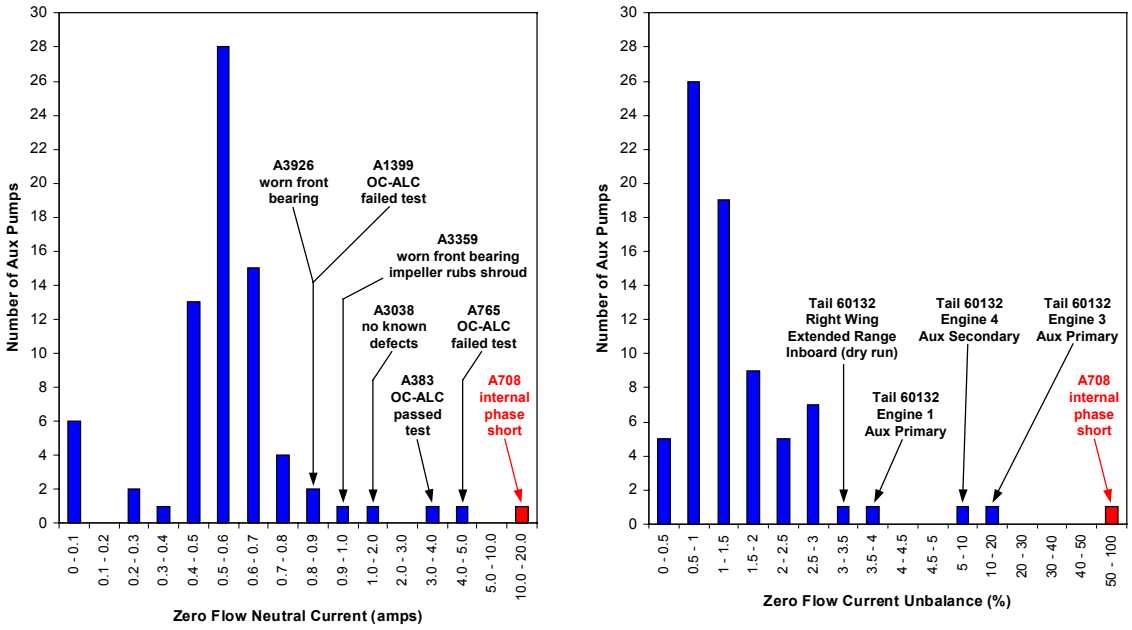

Figure 31: *Distribution of neutral current (left) and current unbalance (right) for all tested auxiliary fuel pumps at zero flow.*

Finally, Figure 32 is presented to show motor speed and motor current for all auxiliary pumps tested at zero flow. The relationship between these two parameters is sensitive to changes in running load that can occur for many reasons, such as inadvertent flow (e.g., from leakage between the pump and scroll housing), lack of fuel (dry running), and friction or binding due to mechanical degradations.

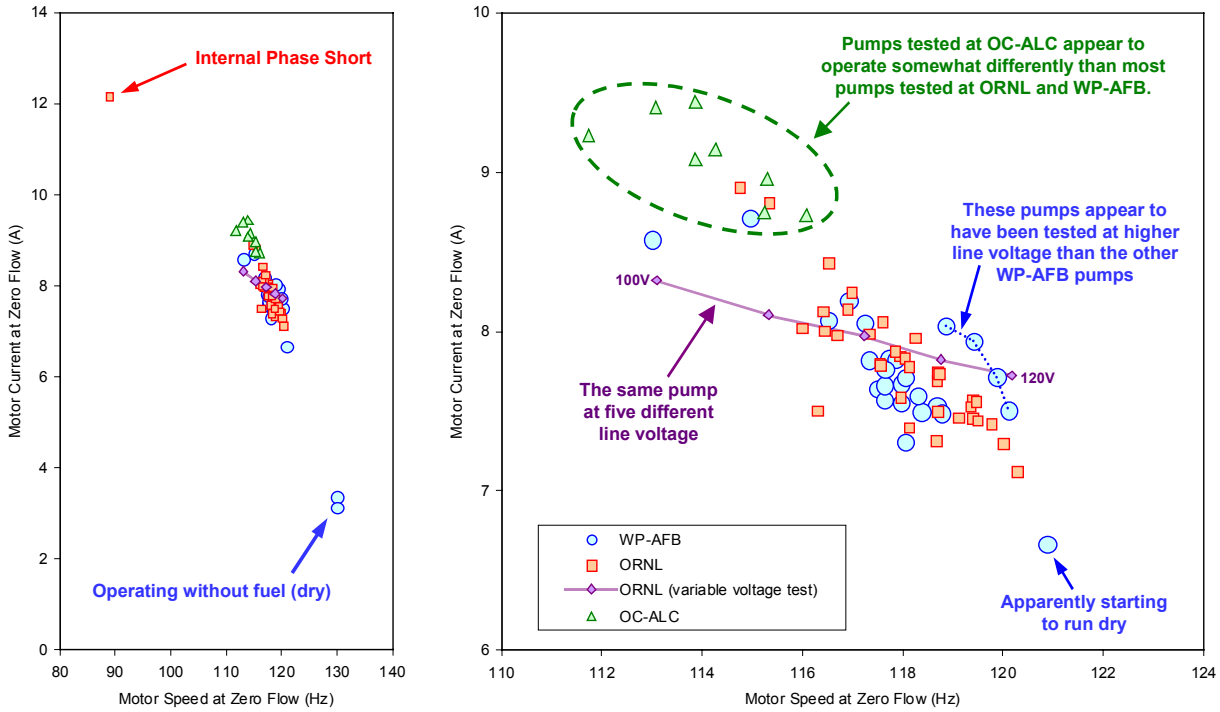

Figure 32: *Motor current and motor speed relationships for all auxiliary fuel pumps tested at zero flow.*

Several points can be made by this one figure:

- Most pumps are generally grouped together, while the outliers represent undesirable conditions: one pump having an internal phase short and two pumps operating without fuel (dry).
- The fuel pumps tested at OC-ALC appear to operate somewhat differently than most pumps tested at ORNL and WP-AFB. This will be investigated further.
- Changes in line voltage for a given pump operating at zero flow will result in a shift in the motor speed vs. current relationship. Line variations produce a pump response that may be distinguished from a load variation.
- Four pumps tested at WP-AFB appear to have been tested at slightly higher (~5 V) line voltage than most other pumps. These pumps had been tested on an aircraft in the flight line, rather than on aircraft in the hanger, as other pumps were.
- Although all tests were supposedly performed at zero flow, the scatter between the data suggests that some pumps may have had fuel leaking between the pump housing and the scroll housing, or may have had mechanical problems. In either case, the motor loading would have increased, resulting in increased current and lower running speed. These effects will also be investigated further.

Conclusions

This paper has described electrical signature analysis (ESA), a powerful technology for condition monitoring, diagnostics, and prognostics of electro-mechanical equipment. ESA is a non-intrusive technology that exploits the abilities of electric motors and generators to act as transducers. As such, the motors and generators provide signals that are similar to those provided by accelerometers. By using a multitude of signal processing and signature analysis techniques, one can use ESA to enhance equipment safety, reliability, and operational readiness by providing improved diagnostics and prognostics.

Oak Ridge National Laboratory is presently developing a portable ESA-based instrument for monitoring the condition of C-141 fuel pumps. During this project fuel pump electric current data have been acquired from many pumps that were tested at WP-AFB, OC-ALC, and at a flow loop in Oak Ridge that was developed during this project. While data have been obtained on both main and auxiliary fuel pumps, the data analysis efforts to-date have focused on the auxiliary fuel pump.

Many auxiliary pumps were obtained from AMARC, carefully inspected, and tested in the ORNL flow loop. In addition to examining and testing auxiliary fuel pumps in their "as received" state, five of these pumps were further degraded with 0.010-inches of additional front bearing wear and retested. Considerable data analyses led to the development of a new capability for detecting front bearing wear in C-141 auxiliary fuel pumps based on the measurement of the demodulated motor current spectrum noise floor obtained at zero flow. This new method appears to offer a reliable means of detecting excessive front bearing wear on pumps tested in flow test facilities and on C-141 aircraft. Motor electrical failures have also been easily detected.

While much has been accomplished during this project, several activities are ongoing or planned for the near future. These activities include:

- Testing of auxiliary fuel pumps is continuing. Methods for detecting additional motor and pump degradations using ESA will be developed.
- A comprehensive test plan will be carried out on main fuel pumps for the purpose of identifying ESA diagnostic methods for these pumps.
- Data acquisition and analysis software will be consolidated and updated with new ESA-based diagnostic methods as they are developed. The final software will be easy to use and provide on-line, immediate assessment of fuel pump condition.
- A suitcase-style ESA instrument is under development. Two prototypes will be constructed and delivered to the Air Force at the conclusion of the project.
- Additional tests will be carried out to understand the differences between the OC-ALC data and data obtained at ORNL and WP-AFB.
- Additional opportunities for developing ESA diagnostic systems will be explored with the Air Force and other interested organizations.

These activities and others will be guided by the same approach identified earlier (see Figure 19) and should result in an effective condition monitoring system for the Air Force C-141 aircraft fuel booster pumps. The platform created by this project should also be amenable to other applications such as fuel pumps on other aircraft and on additional components and systems used by the Air Force and other interested organizations.

References

[1] H. D. Haynes, *Aging and Service Wear of Electric Motor-Operated Valves Used in Engineered Safety-Feature Systems of Nuclear Power Plants - Volume II, Aging Assessments and Monitoring Method Evaluations*, NUREG/CR-4234 Volume 2, Oak Ridge National Laboratory, August, 1989.

[2] Haynes, et al., U.S. Patent number 4965513, *Motor current signature analysis method for diagnosing motor operated devices*. Issued October 23, 1990.

[3] Dickens, et al., U.S. Patent number 5483833, *A method and apparatus for monitoring rotating aircraft components*. Issued January 16, 1996.